JOURNAL OF THEORETICAL AND APPLIED MECHANICS
47, 1, pp. 17-40, Warsaw 2009

AN INFLUENCE MATRIX TECHNIQUE FOR MULTI-DOMAIN SOLUTION OF THE NAVIER-STOKES EQUATIONS IN A VORTICITY-STREAMFUNCTION FORMULATION

Andrzej Bogusławski

Czestochowa University of Technology, Institute of Thermal Machinery, Częstochowa, Poland
e-mail: abogus@imc.pcz.czest.pl

Sławomir Kubacki

Czestochowa University of Technology, Institute of Thermal Machinery, Częstochowa, Poland;
Ghent University, Deptartment of Flow, Heat and Combustion Mechanics, Ghent, Belgium
e-mail: slawomir.kubacki@ugent.be

The paper presents new multi-domain algorithms based on the influence matrix technique applied together with the non-overlapping iterative domain decomposition method for solution of the incompressible Navier-Stokes equations in vorticity-streamfunction formulation. The spectral Chebyshev collocation method and the influence matrix algorithm are applied for solution of the Stokes problem in each subdomain resulting from time discretization of the Navier-Stokes equations, while the patching conditions (continuity of the solution and continuity of its first order derivative) at the interfaces between subdomains are satisfied using the iterative domain decomposition algorithm.

Key words: spectral methods, domain decomposition method, influence matrix technique

1. Introduction

The spectral methods can be effectively used for accurately solution of many complex flows involving evolution of very fine structures and instabilities at sufficiently low Reynolds numbers. Application of these methods to solution of many technical problems is however limited as simple geometry flows can only be considered.

The multi-domain algorithms allows one to extend the applicability of spectral methods to more complex geometry problems where the original computational geometry can be decomposed into smaller subdomains which can be easily transformed into rectangular geometries in the computational space. The accuracy of the solution can also be improved in the case of stiff or singular problems (Peyret, 2002), where the local size of subdomains and degree of polynomial can be adapted to the local level of stiffness, while the singular problems can easily be handled by shifting the singularity points to the corners of the subdomains. On the other hand, one has to solve complex physical problems like development of flow instabilities in geometries of high aspect ratio (e.g. thermohaline convection in tall cavities), where application of a high-order approximation is strictly recommended (Peyret, 2002). The present paper is devoted to development of a multi-domain algorithm for solution of problems involving computational geometries of a high aspect ratio. Furthermore, an application of the multi-domain technique allows for efficient solution of such problems on parallel computers.

Sabbah and Pasquetti (1998) developed a direct algorithm for multi-domain solution of the Navier-Stokes equations in velocity-pressure variables splitting the computational domain in one space direction into a given number of subdomains N_{el}. The solution to the Rayleigh-Bènard convection in 2D and 3D cavities of a high aspect ratio was considered. Application of the spectral multi-domain algorithm for solution to the 3D problem was presented with one homogeneous direction. The multi-domain procedure was based on the direct influence matrix technique. In order to obtain the solution to the Stokes problem in each subdomain, the "extended influence matrix" method was implemented for computation of the pressure and correction term at the physical boundary of the computational domain as described in Kleiser and Schumann (1980) and Tuckerman (1989). The correction term was introduced into the solution to the Poisson equation for pressure in order to recover the divergence-free velocity field at the boundary of the computational domain. The continuity conditions at the interfaces between subdomains were enforced using the interface influence matrix technique (detailed description of the algorithm can also be found in Peyret (2002)). Since the system of equations resulting from the continuity conditions at the interfaces between subdomains was very large, it was finally solved at each time step using the block-tridiagonal version of the LU decomposition algorithm proposed by Isaacson and Keller (1966).

In Forestier *et al.* (2000), the method presented above was applied for solution of the wakes development in a stratified fluid. Some modifications to the

multi-domain algorithm were presented allowing one to impose free-slip and soft outflow boundary conditions. Application of the multi-domain technique was justified by the necessity of accurate resolution of the flow equations in geometries of high aspect ratio.

Further application of the multi-domain algorithm proposed by Sabbah and Pasquetti (1998) can also be found in Sabbah *et al.* (2001) for solution of the thermohaline convection in the cavity of a high aspect ratio where one of the vertical walls was heated. The multi-domain approach together with the spectral Chebyshev approximation allows one to capture complex physical phenomena like evolution and merging of convective cells in an enclosure.

Raspo (2003) shows application of the direct multi-domain technique for solution to the Navier-Stokes equations in vorticity-streamfunction formulation. The algorithm was applied for solution of the flow in a rotating channel-cavity system of T-shape. The influence matrix method was used for solution to the Stokes problem in each subdomain coupling the vorticity and the streamfunction as well as to impose the continuity conditions at the interfaces. The method was applied for decomposition of the computational domain into four subdomains, and the interface influence matrix was constructed and inverted in the preprocessing step. The algorithm allowed one to extend the applicability of the spectral methods to nonrectangular geometries, where the vorticity singularities were shifted to the corners of subdomains.

In the present paper, two multi-domain applications of the influence matrix method for the solution to the Stokes problem are considered, and they are used together with the iterative domain decomposition method proposed by Louchart *et al.* (1998). In Louchart *et al.* (1998) the iterative algorithm was showed for solution to the natural convection problem and the flow in the inverted Bridgman configuration. Motion of the Boussinesq fluid and the heat transfer process were governed by the Navier-Stokes and energy equations.

The first approach is based on the solution to the Stokes problem at each time step where the global system of equations is used to treat the lack of vorticity boundary conditions at no-slip walls. The system of equations is inverted in the preprocessing step on one processor, while at each time-cycle the solution is obtained from simple matrix products. In the second case, the iterative influence matrix method is considered based on the solution of the local system of equations in each subdomain. The latter approach seems to be well suited for parallel computing using distributed memory systems.

The influence matrix techniques will be applied for solution to the incompressible Navier-Stokes equations in vorticity-streamfunction formulation. This approach has some advantages over the velocity-pressure formulation in

the case of two-dimensional flows as the incompressibility condition is automatically satisfied and the number of variables is smaller.

2. Solution of the Navier-Stokes equations

Motion of a fluid is governed by the incompressible Navier-Stokes equations expressed in the vorticity-streamfunction formulation

$$\begin{aligned} &\partial_t \omega + A(\boldsymbol{V}, \omega) = F + \nu \nabla^2 \omega \\ &\nabla^2 \psi + \omega = 0 \end{aligned} \tag{2.1}$$

where ν is the kinematic viscosity, $A(\boldsymbol{V}, \omega) = \boldsymbol{V} \cdot \nabla \omega$, $\boldsymbol{V} = [u, v]$ is the velocity vector and F is the forcing term. The velocity components u and v are related to the streamfunction ψ by

$$u = \frac{\partial \psi}{\partial y} \qquad v = -\frac{\partial \psi}{\partial x} \tag{2.2}$$

and the vorticity ω is defined as

$$\omega = \frac{\partial v}{\partial x} - \frac{\partial u}{\partial y} \tag{2.3}$$

Equations (2.1) are discretized in time using the semi-implicit second order Adams-Bashforth/Backward Differentiation scheme (Peyret, 2002)

$$\begin{aligned} &\frac{3\omega^{(n+1)} - 4\omega^{(n)} + \omega^{(n-1)}}{2\Delta t} + 2A^{(n)} - A^{(n-1)} = F^{(n+1)} + \nu \nabla^2 \omega^{(n+1)} \\ &\nabla^2 \psi^{(n+1)} + \omega^{(n+1)} = 0 \end{aligned} \tag{2.4}$$

where n denotes the number of time step.

Equations (2.4) consist of the Stokes problem in Ω

$$\nabla^2 \omega - \sigma \omega = f \qquad \nabla^2 \psi = -\omega \tag{2.5}$$

with the boundary conditions on $\partial\Omega$

$$\psi = g \qquad \frac{\partial \psi}{\partial n} = h \tag{2.6}$$

where

$$\omega = \omega^{(n+1)} \qquad \psi = \psi^{(n+1)}$$
$$f = \frac{1}{\nu}\Big(-F^{(n+1)} - \frac{4\omega^{(n)} - \omega^{(n-1)}}{2\Delta t} + 2A^{(n)} - A^{(n-1)}\Big) \tag{2.7}$$

with $\sigma = 3/(2\nu\Delta t)$. Note that $F^{(n+1)}$ term in Eq. (2.7) has only non-zero value for the solution to the natural convection problem discussed later. The values of g and h are defined by

$$g = \int_{s_0}^{s} \boldsymbol{V}_{\partial\Omega} \cdot \boldsymbol{n}\, ds \qquad h = \boldsymbol{V}_{\partial\Omega} \cdot \boldsymbol{t} \tag{2.8}$$

where s is the curviliniear abscissa along $\partial\Omega$ and s_0 corresponds to a given arbitrary fixed point on $\partial\Omega$. $\boldsymbol{n}$ is the outward unit vector normal to boundary $\partial\Omega$ and $\boldsymbol{t}$ is the unit vector tangent to boundary $\partial\Omega$ with clockwise orientation.

For spatial approximation of Eq. (2.5) with boundary conditions (2.6) the spectral collocation method is applied (Canuto *et al.*, 1988; Peyret, 2002) where the Bayliss *et al.* (1994) algorithm is used in order to reduce the round-off errors appearing in calculation of the derivatives using the matrix-vector products. The matrix diagonalization algorithm was applied (Haidvogel and Zang, 1979; Haldenwang *et al.*, 1984) for solution of the algebraic system of equations resulting from time discretization of the Navier-Stokes equations.

3. Influence matrix method for solution of the monodomain problem

The influence matrix technique is applied to treat the lack of boundary conditions for the vorticity at the boundary $\partial\Omega$ of the computational domain Ω where the solution (ω, ψ) is expressed as a linear combination of the elementary solutions $(\widetilde{\omega}, \widetilde{\psi})$ and $(\overline{\omega}, \overline{\psi})$ (Peyret, 2002)

$$\omega = \widetilde{\omega} + \overline{\omega} \qquad \psi = \widetilde{\psi} + \overline{\psi} \tag{3.1}$$

where $(\widetilde{\omega}, \widetilde{\psi})$ are the solutions to the following $\widetilde{P}$-problem

$$\begin{aligned} &\nabla^2\widetilde{\omega} - \sigma\widetilde{\omega} = f \qquad \text{in} \quad \Omega \\ &\widetilde{\omega} = 0 \qquad\qquad\qquad\quad \text{on} \quad \partial\Omega^c \end{aligned} \tag{3.2}$$

and

$$\begin{aligned} \nabla^2\widetilde{\psi} &= -\widetilde{\omega} \qquad \text{in} \quad \Omega \\ \widetilde{\psi} &= g \qquad\quad \text{on} \quad \partial\Omega^c \end{aligned} \tag{3.3}$$

where $\partial\Omega^c$ denotes the boundary of the domain Ω without four corner points. The pair $(\overline{\omega}, \overline{\psi})$ is the solution to the $\overline{P}$-problem

$$\left.\begin{aligned} \nabla^2\overline{\omega} - \sigma\overline{\omega} &= 0 \\ \nabla^2\overline{\psi} + \overline{\omega} &= 0 \end{aligned}\right\} \quad \text{in} \quad \Omega \qquad\qquad \left.\begin{aligned} \overline{\psi} &= 0 \\ \partial_n\overline{\psi} &= h - \partial_n\widetilde{\psi} \end{aligned}\right\} \quad \text{on} \quad \partial\Omega^c \tag{3.4}$$

which can be subsequently defined as the $\overline{P}_0$-problem

$$\left.\begin{aligned} \nabla^2\overline{\omega} - \sigma\overline{\omega} &= 0 \\ \nabla^2\overline{\psi} + \overline{\omega} &= 0 \end{aligned}\right\} \quad \text{in} \quad \Omega \qquad\qquad \left.\begin{aligned} \overline{\omega} &= \xi \\ \overline{\psi} &= 0 \end{aligned}\right\} \quad \text{on} \quad \partial\Omega^c \tag{3.5}$$

where the unknown values of ξ (values of ω on the boundary $\partial\Omega^c$) should be determined in such a way that the Neumann condition on $\overline{\psi}$ will be satisfied in Eq. (3.4).

The solutions to (3.5) can be expressed as linear combinations of the elementary solutions $(\overline{\omega}_l, \overline{\psi}_l)$, $l = 1, \ldots, L$

$$\overline{\omega} = \sum_{l=1}^{L} \xi_l \overline{\omega}_l \qquad\qquad \overline{\psi} = \sum_{l=1}^{L} \xi_l \overline{\psi}_l \tag{3.6}$$

where $(\overline{\omega}_l, \overline{\psi}_l)$, $l = 1, \ldots, L$ are the solutions to the following $\overline{P}_l$-problem

$$\begin{aligned} \nabla^2\overline{\omega}_l - \sigma\overline{\omega}_l &= 0 \qquad \text{in} \qquad\qquad \Omega \\ \overline{\omega}_l|_{\eta_j} &= \delta_{jl} \qquad \text{for } \eta_j \in \partial\Omega^c \end{aligned} \tag{3.7}$$

and

$$\begin{aligned} \nabla^2\overline{\psi}_l &= -\overline{\omega}_l \qquad \text{in} \quad \Omega \\ \overline{\psi}_l|_{\eta_j} &= 0 \qquad\quad \text{for} \quad \eta_j \in \partial\Omega^c \end{aligned} \tag{3.8}$$

where η_j, $j = 1, \ldots, 2(N + M - 2)$ are related to the collocation points on the boundary $\partial\Omega^c$ while N and M denote the number of Chebyshev modes in the x- and y-directions, respectively.

Solution to problems (3.7) and (3.8), taking into account Eq. (3.6) and Neumann condition in (3.4), allows one to define the following system of equations for evaluation of the unknown coefficients ξ

$$\sum_{l=1}^{L} (\partial_n\overline{\psi}_l|_{\eta_j})\xi_l = (h - \partial_n\widetilde{\psi})_{\eta_j} \qquad\qquad \eta_j \in \partial\Omega^{c-4} \subset \partial\Omega^c \tag{3.9}$$

for $j = 1, \ldots, L$. The system of equations (3.9) can also be written in the matrix form

$$\mathbf{M}\boldsymbol{\Xi} = \boldsymbol{E} \tag{3.10}$$

where $\mathbf{M}$ is the influence matrix, $\boldsymbol{\Xi} = [\xi_1, \ldots, \xi_L]^\top$ and $\partial\Omega^{c-4}$ denote the boundary $\partial\Omega^c$ without four collocation points. The four equations are eliminated from the system of equations in order to invert the influence matrix $\mathbf{M}$ (Ehrenstein and Peyret, 1989).

It should be noted that the first application of the influence matrix method for solution of the two-dimensional problems was presented by Vanel *et al.* (1986) and Ehrenstein and Peyret (1986). A detailed description of this algorithm can also be found in Peyret (2002).

4. Multi-domain formulation

Taking into account Eq. (3.2) and assuming decomposition of the computational domain into N_{el} subdomains in the x-direction (Fig. 1), the solutions (ω_m, ψ_m) can be expressed in each subdomain Ω_m, $m = \{L, I_k, R\}$, for $k = 1, \ldots, N_{el}^I$ (where $N_{el}^I = N_{el} - 2$) as follows

$$\omega_m = \widetilde{\omega}_m + \overline{\omega}_m \qquad \psi_m = \widetilde{\psi}_m + \overline{\psi}_m \tag{4.1}$$

where $(\widetilde{\omega}_m, \widetilde{\psi}_m)$ are solutions to the $\widetilde{P}_m$-problem

$$\begin{aligned} &\nabla^2\widetilde{\omega}_m - \sigma\widetilde{\omega}_m = f \qquad \text{in} \quad \Omega_m \\ &\widetilde{\omega}_m = 0 \qquad\qquad\qquad\quad \text{on} \quad \partial\Omega_m^c \end{aligned} \tag{4.2}$$

and

$$\begin{aligned} &\nabla^2\widetilde{\psi}_m = -\widetilde{\omega}_m \qquad \text{in} \quad \Omega_m \\ &\widetilde{\psi}_m = g \qquad\qquad\quad \text{on} \quad \partial\Omega_m^c \end{aligned} \tag{4.3}$$

where $\partial\Omega_m^c$ denotes physical boundaries of the subdomains Ω, $m = \{L, I_k, R\}$, for $k = 1, \ldots, N_{el}^I$ without four corner points, while at the interfaces Γ_{L,I_1}, $\Gamma_{k,k+1}$, $k = 1, \ldots, N_{el}^I - 1$, $\Gamma_{I_{N_{el}^I},R}$ between subdomains the following patching conditions are specified

$$\frac{\partial\varphi}{\partial n}_m = \frac{\partial\varphi}{\partial n}_q \qquad \text{and} \qquad \varphi_m = \varphi_q \tag{4.4}$$

where $\varphi = \widetilde{\omega}, \widetilde{\psi}$, n is the normal to the interface between the subdomains Ω_m and Ω_q where $m = \{L, I_k, I_{N_{el}^I}\}$ and $q = \{I_1, I_{k+1}, R\}$ for $k = 1, \ldots, N_{el}^I - 1$ (as shown in Fig. 1). Patching requirements (4.4) are satisfied applying the iterative domain decomposition algorithm proposed by Louchart *et al.* (1998).

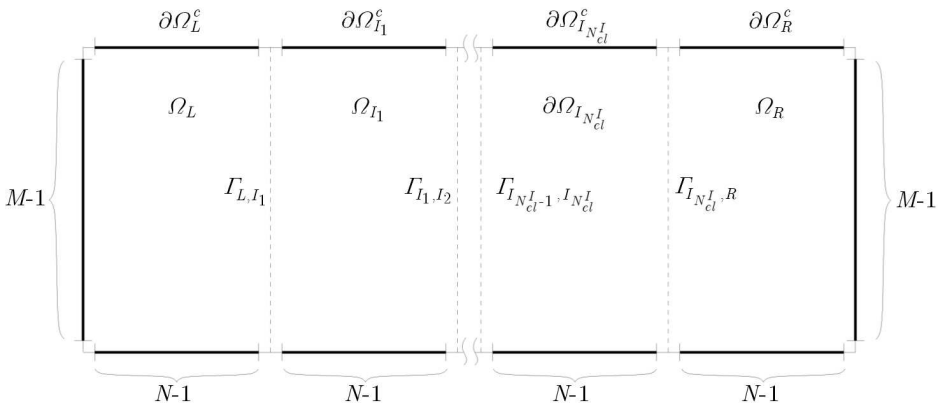

Fig. 1. Scheme of domain decomposition into N_{el} subdomains

The solutions $\overline{\omega}_m$ can be expressed in each subdomain Ω_m, $m = \{L, I_k, R\}$, for $k = 1, \ldots, N_{el}^I$ as a linear combination of the elementary solutions $(\overline{\omega}_{m,l}^p, \overline{\psi}_{m,l}^p)$, $p = \{L, I_k, R\}$ for $k = 1, \ldots, N_{el}^I$ (Kubacki, 2005)

$$\begin{aligned} \overline{\omega}_m &= \sum_{l=1}^{L_L} \xi_l^L \overline{\omega}_{m,l}^L + \sum_{k=1}^{N_{el}^I} \sum_{l=1}^{L_{I_k}} \xi_l^{I_k} \overline{\omega}_{m,l}^{I_k} + \sum_{l=1}^{L_R} \xi_l^R \overline{\omega}_{m,l}^R \\ \overline{\psi}_m &= \sum_{l=1}^{L_L} \xi_l^L \overline{\psi}_{m,l}^L + \sum_{k=1}^{N_{el}^I} \sum_{l=1}^{L_{I_k}} \xi_l^{I_k} \overline{\psi}_{m,l}^{I_k} + \sum_{l=1}^{L_R} \xi_l^R \overline{\psi}_{m,l}^R \end{aligned} \tag{4.5}$$

where $L_L = L_R = 2(N-1) + (M-1)$ and $L_{I_k} = 2(N-1)$ are related to the collocation points respectively on the boundaries $\partial\Omega_L^c$, $\partial\Omega_R^c$ and $\partial\Omega_{I_k}^c$ for $k = 1, \ldots, N_{el}^I$, and the elementary solutions $(\overline{\omega}_{m,l}^p, \overline{\psi}_{m,l}^p)$ satisfy the following problems

$$\begin{aligned} &\nabla^2 \overline{\omega}_{m,l}^p - \sigma \overline{\omega}_{m,l}^p = 0 \qquad \text{in} \quad \Omega_m \\ &\overline{\omega}_{m,l}^p\big|_{\eta_j^{L_p}} = \delta_{jl} \qquad \text{for} \quad \eta_j^{L_p} \in \partial\Omega_p^c \end{aligned} \tag{4.6}$$

and

$$\begin{aligned} &\nabla^2 \overline{\psi}_{m,l}^p = -\overline{\omega}_{m,l}^p \qquad \text{in} \quad \Omega_m \\ &\overline{\psi}_{m,l}^p\big|_{\eta_j^{L_p}} = 0 \qquad \text{for} \quad \eta_j^{L_p} \in \partial\Omega_p^c \end{aligned} \tag{4.7}$$

where: $p = \{L, I_k, R\}$ for $k = 1, \ldots, N_{el}^I$, while $j = 1, \ldots, L_*$ assuming that $L_* = L_L$ if $p = L$, $L_* = L_{I_k}$ if $p = I_k$ for $k = 1, \ldots, N_{el}^I$ and $L_* = L_R$ if $p = R$, where at the interfaces Γ_{L,I_1}, $\Gamma_{k,k+1}$, $k = 1, \ldots, N_{el}^I - 1$, $\Gamma_{I_{N_{el}^I},R}$ patching conditions (4.4) should be satisfied taking $\varphi = \overline{\omega}_{m,l}^p, \overline{\psi}_{m,l}^p$. As it is seen, the number of solutions (4.6) and (4.7) becomes very large splitting the computational domain into a higher number of subdomains, however it should be noted that these solutions can be set up in the preliminary calculation before time integration, and can be stored in memory until the influence matrix is formulated.

Finally, assuming that the Neumann boundary condition should be fulfilled in Eq. (3.4) and knowing that $\overline{\psi}_m$ is defined by Eq. $(4.5)_2$, the unknown values of the coefficients ξ can be obtained by solving the following system of equations

$$\sum_{l=1}^{L_L} (\partial_n \overline{\psi}_{m,l}^L|_{\eta_j^{Lm}}) \xi_l^L + \sum_{k=1}^{N_{el}^I} \sum_{l=1}^{L_{I_k}} (\partial_n \overline{\psi}_{m,l}^{I_k}|_{\eta_j^{Lm}}) \xi_l^{I_k} + \sum_{l=1}^{L_R} (\partial_n \overline{\psi}_{m,l}^R|_{\eta_j^{Lm}}) \xi_l^R =$$
$$= (h_m - \partial_n \widetilde{\psi}_m)_{\eta_j^{Lm}} \qquad \eta_j^{Lm} \in \partial\Omega_{G-4}^c \subset \partial\Omega_G^c \tag{4.8}$$

for $j = 1, \ldots, L_m$, $m = \{L, I_k, R\}$, $k = 1, \ldots, N_{el}^I$.

System (4.8) can also be written in the following matrix form

$$\mathbf{M}_G \boldsymbol{\Xi}_G = \boldsymbol{E}_G \tag{4.9}$$

where $\mathbf{M}_G$ is the influence matrix, $\boldsymbol{\Xi}_G = [\xi_1, \ldots, \xi_{L_G}]^\top$ and $\partial\Omega_{G-4}$ denotes the physical boundary $\partial\Omega_G$ without four collocation points which are removed from the system of equations in order to invert the influence matrix $\mathbf{M}_G$. The singular nature of the influence matrix was discussed in Ehrenstein and Peyret (1989). In the present algorithm, the singularity of system (4.8) was removed eliminating four collocation points located close to the corners of the domain Ω (Ehrenstein and Peyret, 1989). As algorithm (4.9) involves all collocation points on the boundary $\partial\Omega$ it will be named the global influence matrix method (for short GIM method).

Summing up, the multi-domain algorithm based on the global influence matrix is as follows:

1. Preprocessing stage:

   (a) Solution to problems (4.6) and (4.7) using the iterative domain decomposition method (Louchart *et al.*, 1998) taking into account

patching conditions (4.4) and storing the solutions $(\overline{\omega}^p_{m,l}, \overline{\psi}^p_{m,l})$, $p = \{L, I_k, R\}$, $k = 1, ..., N^I_{el}$ in each subdomain Ω_m, $m = \{L, I_k, R\}$, for $k = 1, \ldots, N^I_{el}$.

(b) Formulation of the global influence matrix $\mathbf{M}_G$ on the master processor, inversion of this matrix and storage of the inverse.

2. At each time step:

(a) Calculation of the right-hand side f in Eq. (4.2).

(b) Solution to the $\widetilde{P}_m$-problem (Eqs. (4.2) and (4.3)) using the iterative domain decomposition method (Louchart *et al.*, 1998) taking into account patching conditions (4.4).

(c) Calculation of the right-hand side of Eq. (4.9) – transmission of the data from all processors to the master one.

(d) Computation of the coefficients ξ (Eq. (4.9)) on the master processor by simple matrix-vector multiplication.

(e) Transmission of the coefficients ξ from the master processor to the other ones.

(f) Calculation of the final solution using Eqs. (4.5) and (4.1).

It should be noted that in the present algorithm the influence matrix $\mathbf{M}_G$ was inverted on one processor before time integration, and at each time step an evaluation of the unknown coefficients ξ was obtained by simple matrix-vector multiplication. This method can be however applied for solution of the problems where the decomposition into a limited number of subdomains will be considered, otherwise the communication overheads can increase substantially.

As an alternative, the iterative influence matrix algorithm is proposed based on the solution to the local system of equations in each subdomain Ω_m, $m = \{L, I_k, R\}$, for $k = 1, \ldots, N^I_{el}$. The solution to problems (4.2)-(4.3) and (4.6)-(4.7) is the same as before requiring that patching conditions (4.4) should be fulfilled at the interfaces between subdomains, while Eqs. (4.5) can be defined for the subdomain $(m = L)$ in the following way

$$\begin{aligned}
\overline{\omega}_L &\equiv \sum_{l=1}^{L_L} \gamma_l^{L,(n)} \overline{\omega}^L_{L,l} + \sum_{k=1}^{N^I_{el}} \sum_{l=1}^{L_{I_k}} \gamma_l^{I_k,(n-1)} \overline{\omega}^{I_k}_{L,l} + \sum_{l=1}^{L_R} \gamma_l^{R,(n-1)} \overline{\omega}^R_{L,l} \\
\overline{\psi}_L &\equiv \sum_{l=1}^{L_L} \gamma_l^{L,(n)} \overline{\psi}^L_{L,l} + \sum_{k=1}^{N^I_{el}} \sum_{l=1}^{L_{I_k}} \gamma_l^{I_k,(n-1)} \overline{\psi}^{I_k}_{L,l} + \sum_{l=1}^{L_R} \gamma_l^{R,(n-1)} \overline{\psi}^R_{L,l}
\end{aligned} \tag{4.10}$$

where (n) is the number of iteration steps assuming that the coefficients $\gamma^{p,(n)} = \gamma^p$, $p = \{L, I_k, R\}$, $k = 1, \ldots, N_{el}^I$ as $n \to \infty$. In Eqs. (4.10), the coefficients $\gamma^{I_k,(n-1)}$ and $\gamma^{R,(n-1)}$ related to the subdomains Ω_{I_k} for $k = 1, \ldots, N_{el}^I$ and Ω_R will be taken from the previous iterative step $(n-1)$. Taking into account Eq. $(4.10)_2$ and the Neumann condition in Eq. (3.4), the following system of equations is defined for $n \geqslant 1$ allowing one to obtain the unknown coefficients $\gamma^{L,(n)}$

$$\sum_{l=1}^{L_L} (\partial_n \overline{\psi}_{L,l}^L|_{\eta_j^{L_L}}) \gamma_l^{L,(n)} = (h_L - \partial_n \widetilde{\psi}_L)_{\eta_j^{L_L}} - \sum_{k=1}^{N_{el}^I} \sum_{l=1}^{L_{I_k}} (\partial_n \overline{\psi}_{L,l}^{I_k}|_{\eta_j^{L_L}}) \gamma_l^{I_k,(n-1)} + \tag{4.11}$$

$$- \sum_{l=1}^{L_R} (\partial_n \overline{\psi}_{L,l}^R|_{\eta_j^{L_L}}) \gamma_l^{R,(n-1)} \qquad \eta_j^{L_L} \in \partial\Omega_{L-2}^c \subset \partial\Omega_L^c \qquad j = 1, \ldots, L_L$$

which can also be written in the matrix form

$$\mathbf{M}_L \boldsymbol{\Xi}_L = \boldsymbol{E}_L \tag{4.12}$$

where $\boldsymbol{\Xi}_L = [\gamma_1, \ldots, \gamma_{L_L}]^\top$. In Eq. (4.12), the number of collocation points related to the boundary $\partial\Omega_L^c$ is equal to $L_L = 2(N-1) + (M-1)$ (see Fig. 1), while two collocation points should be removed from the system of equations in order to invert the influence matrix $\mathbf{M}_L$. The singularity of the system is removed in a similar way as proposed by Ehrenstein and Peyret (1989) for solution of the monodomain problem.

Equations (4.10) can be readily defined for other subdomains Ω_{I_k}, $k = 1, \ldots, N_{el}^I$ and Ω_R, while here the systems of equations for computation of the coefficients $\gamma^{p,(n)}$, $p = \{L, I_k, R\}$, $k = 1, \ldots, N_{el}^I$ will be mainly shown.

Next, for each subdomain Ω_{I_k}, $k = 1, \ldots, N_{el}^I$, the following local system of equations is defined

$$\sum_{l=1}^{L_{I_k}} (\partial_n \overline{\psi}_{I_k,l}^{I_k}|_{\eta_j^{L_{I_k}}}) \gamma_l^{I_k,(n)} = (h_{I_k} - \partial_n \widetilde{\psi}_{I_k})_{\eta_j^{L_{I_k}}} - \sum_{l=1}^{L_L} (\partial_n \overline{\psi}_{I_k,l}^L|_{\eta_j^{L_{I_k}}}) \gamma_l^{L,(n-1)} +$$

$$- \sum_{\substack{p=1 \\ (p \neq k)}}^{N_{el}^I} \sum_{l=1}^{L_{I_p}} (\partial_n \overline{\psi}_{I_k,l}^{I_p}|_{\eta_j^{L_{I_k}}}) \gamma_l^{I_p,(n-1)} - \sum_{l=1}^{L_R} (\partial_n \overline{\psi}_{I_k,l}^R|_{\eta_j^{L_{I_k}}}) \gamma_l^{R,(n-1)} \tag{4.13}$$

$$\eta_j^{L_{I_k}} \in \partial\Omega_{I_k}^c \qquad j = 1, \ldots, L_{I_k}$$

which can also be written in the matrix form

$$\mathbf{M}_{I_k} \boldsymbol{\Xi}_{I_k} = \boldsymbol{E}_{I_k} \tag{4.14}$$

where $\boldsymbol{\Xi}_{I_k} = [\gamma_1, \ldots, \gamma_{L_{I_k}}]^\top$. It should be stressed that the influence matrix $\mathbf{M}_{I_k}$ is not singular as only one Neumann boundary condition can be defined at the physical boundary $\partial\Omega^c_{I_k}$, thus the resulting number of equations is equal to $L_{I_k} = 2(N-1)$.

Finally, the following system of equations is defined in the subdomain Ω_R for evaluation of the coefficients $\gamma^{R,(n)}$

$$\sum_{l=1}^{L_R} (\partial_n \overline{\psi}^R_{R,l}\big|_{\eta_j^{L_R}})\gamma_l^{R,(n)} = (h_R - \partial_n \widetilde{\psi}_R)_{\eta_j^{L_R}} - \sum_{l=1}^{L_L} (\partial_n \overline{\psi}^L_{R,l}\big|_{\eta_j^{L_R}})\gamma_l^{L,(n-1)} + \\ - \sum_{k=1}^{N^I_{el}} \sum_{l=1}^{L_{I_k}} (\partial_n \overline{\psi}^{I_k}_{R,l}\big|_{\eta_j^{L_R}})\gamma_l^{I_k,(n-1)} \qquad \begin{array}{l} \eta_j^{L_R} \in \partial\Omega^c_{R-2} \subset \partial\Omega^c_R \\ j = 1, \ldots, L_R \end{array} \tag{4.15}$$

or equivalently

$$\mathbf{M}_R \boldsymbol{\Xi}_R = \boldsymbol{E}_R \tag{4.16}$$

where $\boldsymbol{\Xi}_R = [\gamma_1, \ldots, \gamma_R]^\top$ knowing that the number of collocation points on the boundary $\partial\Omega^c_R$ is equal to $L_R = 2(N-1) + (M-1)$. Similarly as for Ω_L, the influence matrix $\mathbf{M}_R$ is singular as two eigenvalues are equal to zero. The singularity was removed by removing two equations related to the collocation points located close to the corners of the physical boundary $\partial\Omega^c_R$ (Ehrenstein and Peyret, 1989).

Further, in order to avoid some convergence difficulties using the iterative influence matrix method, new coefficients $\widehat{\gamma}^{p,(n)}$, $p = \{L, I_k, R\}$ can be computed for the next iterative step $(n+1)$ using the relaxation formula shown below (after solving of Eqs. (4.12), (4.14) and (4.16))

$$\widehat{\gamma}^{p,(n+1)} = \theta \gamma^{p,(n)} + (1-\theta)\widehat{\gamma}^{p,(n)} \tag{4.17}$$

where $0 < \theta \leqslant 1$ is the relaxation factor.

Summing up, the multi-domain algorithm based on the iterative influence matrix method is as follows:

1. Preprocessing stage:

   (a) Solution to problems (4.6) and (4.7) using the iterative domain decomposition method (Louchart *et al.*, 1998) taking into account patching conditions (4.4) and storing the solutions $(\overline{\omega}^p_{m,l}, \overline{\psi}^p_{m,l})$, $p = \{L, I_k, R\}$, $k = 1, \ldots, N^I_{el}$ in each subdomain Ω_m, $m = \{L, I_k, R\}$, for $k = 1, \ldots, N^I_{el}$.

(b) Formulation of the local influence matrices $\mathbf{M}_L$, $\mathbf{M}_{I_k}$ for $k = 1, \ldots, N_{el}^I$ and $\mathbf{M}_R$ in each subdomain Ω_m, $m = \{L, I_k, R\}$, for $k = 1, \ldots, N_{el}^I$ (Eqs. (4.12), (4.14) and (4.16)), their inversion and storing the inverses.

2. At each time step:

(a) Calculation of the right-hand side f in Eqs. (4.2).

(b) Solution to the $\widetilde{P}_m$-problem (Eqs. (4.2) and (4.3)) using the iterative domain decomposition method (Louchart *et al.*, 1998) taking into account patching conditions (4.4).

(c) Computation of the coefficients $\widehat{\gamma}^p$ for $p = \{L, I_k, R\}$, $k = 1, \ldots, N_{el}^I$ using the iterative influence matrix method summarized below.

(d) Setting $\xi^p = \widehat{\gamma}^p$ and computing the final solution using Eqs. (4.5) and (4.1).

The iterative influence matrix method based on the local influence matrices can be summarized as follows:

1. Evaluation of the right-hand side of the Eqs. (4.12), (4.14) and (4.16) setting at the first time step the initial values of $\gamma^{p,(n-1)}$, $p = \{L, I_k, R\}$, $k = 1, \ldots, N_{el}^I$ equal to zero.

2. Solution to Eqs. (4.12), (4.14) and (4.16) in each subdomain Ω_m, $m = \{L, I_k, R\}$, for $k = 1, \ldots, N_{el}^I$.

3. Computation of the coefficients $\widehat{\gamma}^{p,(n)}$, $p = \{L, I_k, R\}$, $k = 1, \ldots, N_{el}^I$ using formula (4.17).

4. Transmission of the data ($\widehat{\gamma}^{p,(n)}$, $p = \{L, I_k, R\}$, $k = 1, \ldots, N_{el}^I$) between the subdomains (processors).

5. Computation of the right-hand side of Eqs. (4.12), (4.14) and (4.16) for the next iteration step replacing the values of $\gamma^{p,(n)}$ by $\widehat{\gamma}^{p,(n)}$, $p = \{L, I_k, R\}$, $k = 1, \ldots, N_{el}^I$.

6. Repeating steps from 2 to 5 until convergence is obtained.

The iterative algorithm based on the solution to the local influence matrices will be named the local influence matrix method (LIM).

5. Results

The numerical results will be presented for solving two-dimensional problems including driven cavity flows and the natural convection problem in the cavity of a hight aspect ratio. First, the accuracy of the Navier-Stokes solver will be checked for the solution to the lid- and regularized driven cavity flows in the monodomain case. Next, the accuracy of multi-domain algorithms implementation will be analysed for solution of the driven cavity problems splitting the computational domain into a few subdomains in one space direction coupling the influence matrix method (GIM and LIM methods) and the domain decomposition algorithm by Louchart *et al.* (1998). The application of the multi-domain techniques will also be presented for solving the natural convection problem using the iterative influence matrix method. Lastly, some results concerning the implementation of the algorithms on parallel computers will be presented.

The following error ϵ_Γ is computed based on the errors ϵ_Γ^m computed at the interfaces between subdomains using the iterative domain decomposition algorithm by Louchart *et al.* (1998)

$$\begin{aligned} \epsilon_\Gamma &= \max(\epsilon_\Gamma^{m,q}) \\ \epsilon_\Gamma^{m,q} &= \frac{\max[\varphi^{(n)}(\Gamma_{m,q}) - \varphi^{(n-1)}(\Gamma_{m,q})]}{\max[\varphi^{(n)}(\Gamma_{m,q})]} \end{aligned} \tag{5.1}$$

where φ denotes the corresponding solution, $m = \{L, I_k, I_{N_{el}^I}\}$, $q = \{I_1, I_{k+1}, R\}$, $k = 1, \ldots, N_{el}^I - 1$, while for the iterative influence matrix method based on the solution to the local influence matrices the error ϵ_{infl} is computed

$$\epsilon_{infl} = \max(\epsilon_{infl}^m) \qquad \epsilon_{infl}^m = \frac{\max[\gamma_m^{(n)} - \gamma_m^{(n-1)}]}{\max[\gamma_m^{(n)}]} \tag{5.2}$$

where $m = \{L, I_k, R\}$, $k = 1, \ldots, N_{el}^I$. The convergence of the iterative domain decomposition algorithm was obtained assuming $\epsilon_\Gamma < 10^{-8}$.

5.1. Driven cavity problems

In order to check correctness of the present solver implementation using monodomain and multi-domain approaches, mainly two test cases are considered. The first problem concerns the lid-driven cavity flow ($\Omega = [0, a]^2$, $a = 1$)

where the velocity components at the moving side of the cavity are equal to $u = 1$ and $v = 0$, and the second one considers the regularized driven cavity test case where u and v are defined as below (Ehrenstein and Peyret, 1989)

$$u(x,1) = -16x^2(1-x)^2 \qquad v(x,1) = 0 \tag{5.3}$$

while on the other sides of the cavity $u = 0$ and $v = 0$. Equations (2.1) are made dimensionless by using $l_{ref} = a$, $u_{ref} = \max[\mathrm{abs}(u(x,a))] = 1$ and $t_{ref} = l_{ref}/u_{ref}$ as the reference length, velocity and time, respectively.

Figure 2 shows the profiles of two velocity components at the vertical and horizontal centrelines of the cavity obtained for the solution to the lid-driven cavity flow at various Reynolds numbers. The present results obtained using the spectral collocation method are compared with the benchmark results of Ghia *et al.* (1982), where the central-difference scheme was applied. In the computations by Ghia *et al.* (1982) a fine computational mesh was used consisting of $N = M = 129$ grid points, while in the current computations the number of collocation points was equal to $N = M = 24$ for $Re = 100$ and $Re = 400$, while for $Re = 1000$, $N = M = 30$. Both results are in good agreement.

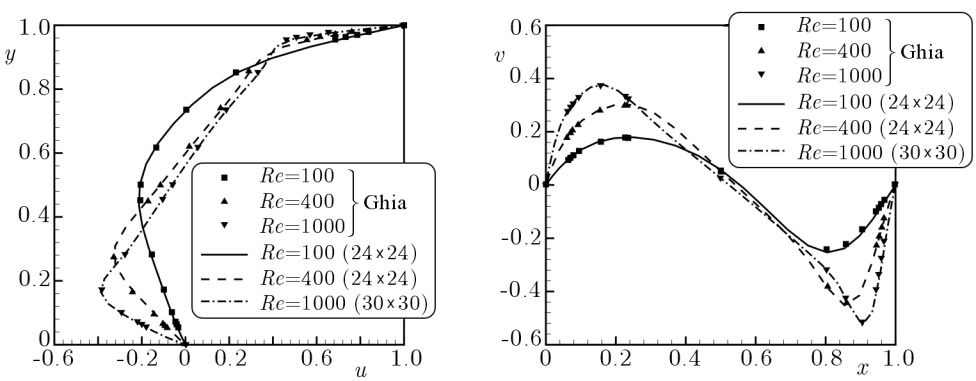

Fig. 2. Velocity profiles of u- (left) and v-velocity (right) components at centrelines of the cavity (lid-driven cavity problem)

For the regularized driven cavity problem, the following parameters $M_1 = \max(\psi_{i,j})$ and $M_2 = \max(\omega_{i,j})$ are determined at the collocation points. Table 1 shows a comparison of these parameters as well as their localization in the computational domain with the literature data of Ehrenstein and Peyret (1989) and Hugues and Randriamampianina (1998). It should be noted that in Ehrenstein and Peyret (1989), the similar influence matrix method was applied for solution of the $\psi - \omega$ equations as in the present case, while in Hugues

and Randriamampianina (1998), the projection method was used for solution of the incompressible Navier-Stokes equations in the velocity-pressure formulation. The values of M_1 and M_2 obtained using the present algorithm agree

Table 1. Influence of the grid resolution $(N = M)$ on M_1 and M_2 for the regularized driven cavity problem $(Re = 400)$. Localization of these quantities is shown in brackets (for M_2 on the top side of the cavity $y = 1$). The literature data of Ehrenstein and Peyret (1989) and Hugues and Randriamampianina (1998) are denoted respectively by EP and HR

$N = M$	M_1	M_2	M_1^{EP}	M_2^{EP}	M_1^{HR}	M_2^{HR}
16	8.5379E-02 (0.40, 0.60)	25.2328 (0.60)	8.5378E-02 (0.40, 0.60)	25.2329 (0.60)	8.5979E-02 (0.40, 0.60)	25.0387 (0.60)
20	8.5213E-02 (0.42, 0.58)	24.6692 (0.65)	8.5213E-02 (0.43, 0.58)	24.6693 (0.65)	8.5185E-02 (0.42, 0.58)	24.6404 (0.65)
24	8.5716E-02 (0.43, 0.63)	24.9343 (0.63)	8.5716E-02 (0.43, 0.63)	24.9344 (0.63)	8.5718E-02 (0.43, 0.63)	24.9333 (0.63)
32	8.5481E-02 (0.40, 0.60)	24.7844 (0.65)	8.5480E-02 (0.40, 0.60)	24.7845 (0.60)	8.5481E-02 (0.40, 0.60)	24.7844 (0.65)

within 0.001% with the results of Ehrenstein and Peyret (1989) and within 0.8% with the data of Hugues and Randriamampianina (1998). Localizations of the maxima are the same as shown in Ehrenstein and Peyret (1989) and Hugues and Randriamampianina (1998). This confirms the correctness of the influence matrix implementation in the monodomain case.

For the lid-driven cavity problem, a comparison of the profiles of the u-velocity components at the vertical centreline of the cavity for monodomain and multi-domain cases assuming various Reynolds numbers is shown in Fig. 3. In the multi-domain case, the domain decomposition algorithm together with the GIM method was used by splitting the domain Ω into two and four subdomains. The results obtained for the solution of the monodomain problem and using the multi-domain technique are in good agreement and confirm the correctness of the iterative domain decomposition and influence matrix methods implementation.

Table 2 shows values of M_1 and M_2 and their localization in the computational domain Ω applying the GIM and LIM methods splitting the computational domain into three subdomains. The solutions were obtained assuming different numbers of Chebyshev modes (N) in the x-direction. For the iterative influence matrix method, the value of $\epsilon_{infl} < 10^{-5}$. As it can be seen, the values of these quantities are close to each other and their localizations are identical.

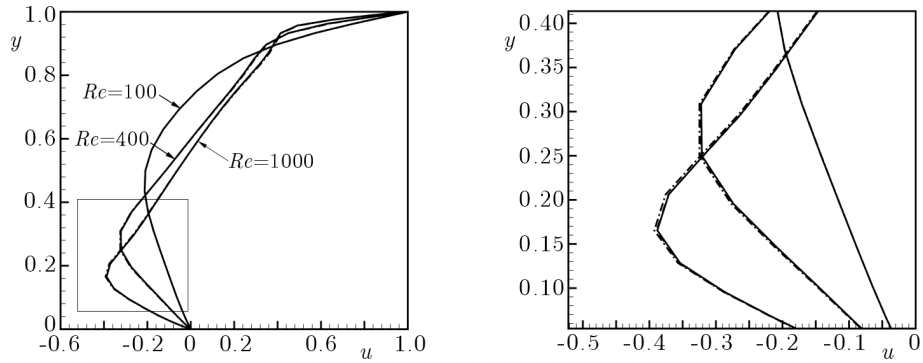

Fig. 3. Velocity profiles of the u-velocity component at the vertical centreline of the cavity for various Reynolds numbers (left) and magnified view (right). Solid line – one domain; dashed line – two subdomains; dased-dotted line – four subdomains

Table 2. Values of M_1 and M_2 and localization of these quantities (in brackets) for solution of the regularized driven cavity flow applying the GIM and LIM algorithms splitting the computational domain into three subdomains ($Re = 400$)

M	N	M_1^{GIM}	M_2^{GIM}	M_1^{LIM}	M_2^{LIM}
24	8	8.4723E-02 (0.44, 0.63)	24.9272 (0.62)	8.4723E-02 (0.44, 0.63)	24.9286 (0.62)
24	10	8.6075E-02 (0.40, 0.63)	24.8974 (0.63)	8.6074E-02 (0.40, 0.63)	24.8999 (0.63)
24	12	8.5848E-02 (0.42, 0.63)	24.8932 (0.62)	8.5848E-02 (0.42, 0.63)	24.8951 (0.62)

5.2. Natural convection in tall cavity

As the next example, the solution to the natural convection in the computational geometry of high aspect ratio is considered, where the multi-domain approach is implemented along the direction of high length. The heat transfer process and fluid motion are governed by the following energy and Navier-Stokes equations within the Boussinesq approximation

$$\begin{aligned} &\partial_t T + \boldsymbol{V} \cdot \nabla T = \nabla^2 T \\ &\partial_t \omega + A(\boldsymbol{V}, \omega) = F + Pr \nabla^2 \omega \\ &\nabla^2 \psi + \omega = 0 \end{aligned} \tag{5.4}$$

where the dimensionless temperature is defined as $T = (\widehat{T} - \widehat{T}_{cold})/\Delta\widehat{T}$, $\Delta\widehat{T} = (\widehat{T}_{hot} - \widehat{T}_{cold}) > 0$ and the body force $F = -RaPr\partial_x T$ where Ra and Pr are the Rayleigh and Prandtl numbers

$$Ra = \frac{g\alpha_T \Delta\widehat{T} l_{ref}^3}{\kappa_T \nu} \qquad Pr = \frac{\nu}{\kappa_T} \tag{5.5}$$

The Navier-Stokes equations are normalized by taking as the reference length, time and velocity the following values respectively $l_{ref} = W/2$, where W is the width of the cavity, and $t_{ref} = l_{ref}^2/\kappa_T$ and $u_{ref} = \kappa_T/l_{ref}$. κ_T is the thermal diffusivity, α_T is the thermal expansion coefficient and g is the gravitational acceleration. The scheme of computational geometry is shown in Fig. 4, where the horizontal walls are assumed to be adiabatic and the vertical ones are maintained at constant temperatures set to zero at the left side and to one at the right one. The gravitational acceleration acts parallelly to the walls kept at constant temperatures. All velocity components are equal to zero at the boundaries of the computational domain. The value of ϵ_{infl} was set to be $\epsilon_{infl} < 10^{-4}$ and $\theta = 0.9$ in Eq. (4.17).

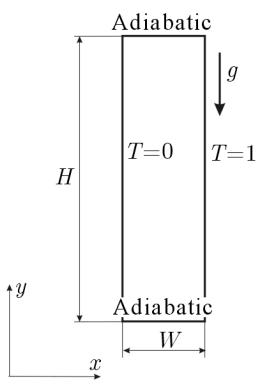

Fig. 4. Scheme of the computational domain for natural convection problem and the boundary conditions for temperature

Figure 5 shows the results obtained using the LIM method, where the computational domain was split into $N_{el} = 10$ subdomains following the y-direction (taking the same number of processors). Temporal evolution of the flow structures can be observed during transient stages where the flow starts to develop from the monocellular case characterised by the conduction regime. In the successive time steps, when the convection becomes dominant, different flow behavior can be seen before the five-cell structure is formed at the final state.

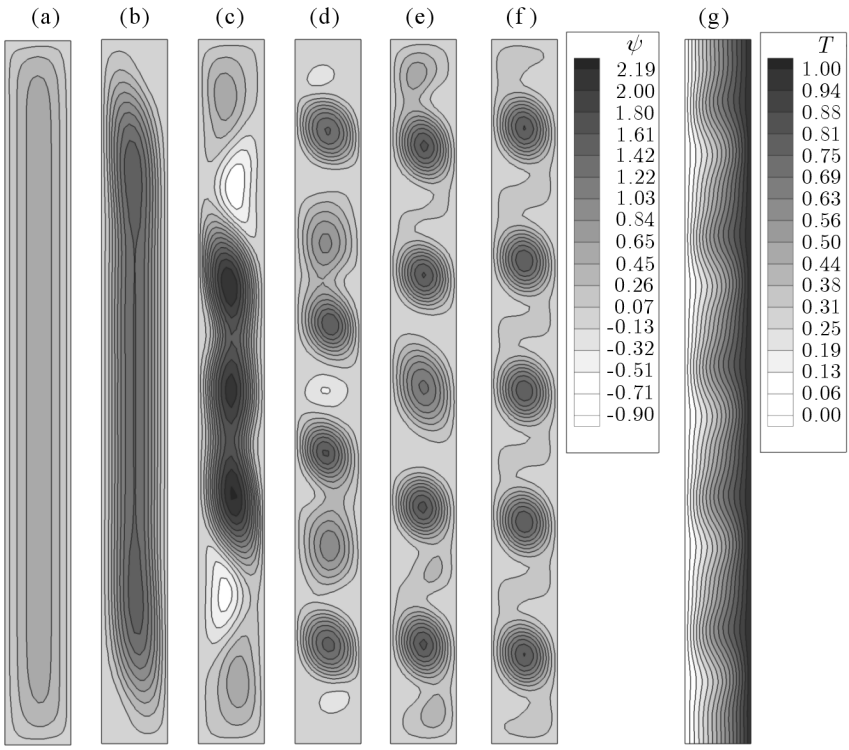

Fig. 5. (a-f) Iso-stream function contours during the transient stage and (g) the temperature field at the final stage for $AR = 10$ and $N_{el} = 10$, using $N = M = 20$ in each subdomain, $\Delta t = 0.0005$ at $Ra = 1000$, $Pr = 0.01$

It should be stressed that only few iterative steps were necessary in order to obtain converged solutions for $\widetilde{\psi}$ and T at each time step, while about 30 iterative steps were necessary for $\widetilde{\omega}$ using the iterative domain decomposition algorithm (Louchart *et al.*, 1998). This confirms the observations reported in Louchart *et al.* (1998) and in Louchart and Randriamampianina (2000) where the same iterative algorithm was applied for solution of the Navier-Stokes equations in the velocity-pressure formulation. It was showed in Louchart and Randriamampianina (2000) that only two iteration steps were necessary in order to obtain a converged solution for the variables having Dirichlet or mixed boundary conditions, while for the pressure the number of iteration steps was higher increasing the number of subdomains due to the Neumann boundary conditions. In the present work, the number of iteration steps does not change significantly increasing the number of subdomains as the Dirichlet and mixed boundary conditions were only involved for solution of the energy and the

Navier-Stokes equations in the vorticity-streamfunction formulation, however a much higher number of iterations was required for $\widetilde{\omega}$ than for the other variables.

5.3. Parallel performance

Figure 6 (left) shows the speed-up (S) obtained running the iterative domain decomposition algorithm on N_p processors. It is defined as the ratio of the computational time t_1 executing the parallel program on a single processor to the time t_p obtained on N_p processors, $S = t_1/t_p$. The speed-up obtained applying the iterative domain decomposition algorithm proposed by Louchart *et al.* (1998) was measured for solving of the 2D Helmholtz equation

$$\begin{aligned} -\nabla^2 u_m + \sigma u_m &= f \qquad \text{in} \quad \Omega_m \\ u_m &= 0 \qquad\qquad\ \text{on} \quad \partial\Omega_m \backslash \Gamma \end{aligned} \tag{5.6}$$

since the same type of equation is solved at each time-cycle using the presented above time discretization scheme (Eqs. (4.2)-(4.3), (4.6)-(4.7)), with the same patching conditions (4.4) specified at the interfaces between subdomains Ω_m. The constant σ was equal to unity, while the right-hand side of the Eq. (5.6) was computed in such a way that $u = \sin(\pi x/(a+b))\sin(\pi y)$ for $\Omega = (a,b) \times (0,1)$, $a = 0$, $b = 0.5N_{el}$. The tests have been performed on the PC-cluster of the Linux system with the Fast Ethernet network. The communication between processors was established using MPI standard libraries.

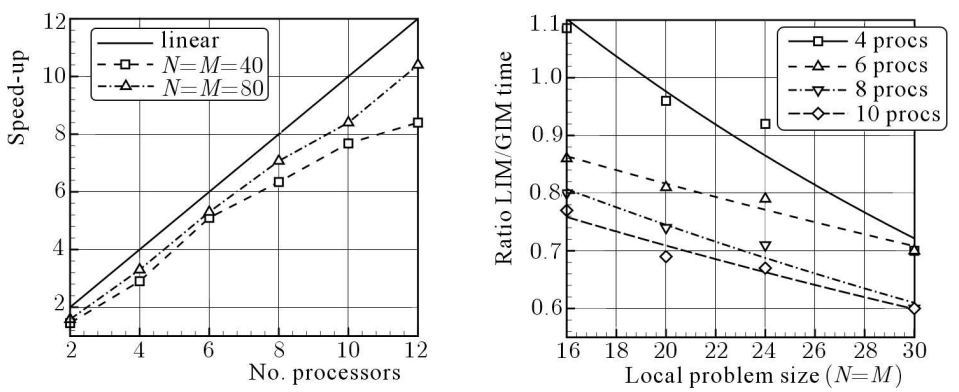

Fig. 6. (left) Speed-up obtained using the Louchart *et al.* (1998) algorithm and (right) ratio of the computational time obtained using the LIM and GIM algorithms

As shown, the speed-up obtained running the parallel algorithm on 12 processors is about $S = 8$ for $N = M = 40$ and $S = 10$ for $N = M = 80$. This

confirms good performance of the iterative algorithm proposed by Louchart *et al.* (1998) for solution of the Helmholtz equation on parallel computers.

Comparison of computational costs between the LIM and GIM methods is performed for the natural convection problem running the parallel algorithm on a different number of processors assuming that the number of processors is equal to the number of subdomains. Figure 6 (right) shows the ratio of the computational time obtained using both influence matrix methods assuming a different problem size $(N = M)$ in each subdomain. As it can be seen, running the parallel code on four processors, a smaller computational time is necessary using the GIM method than applying the LIM algorithm if the local problem size is small enough $(N = M = 16)$. It can be explained by the fact that using the GIM algorithm, the unknown coefficients ξ are obtained by simple matrix-vector multiplication which can be performed in an efficient way using the Fortran Library routine. On the other hand, increasing the number of collocation points and the number of subdomains, the execution time can be considerably reduced by applying the iterative method. Running the problem on a higher number of processors (for $N = M = 30$), the time obtained using the LIM method is about 40% smaller than using the GIM algorithm.

The present LIM approach based on solution of the local influence matrices in each subdomain can be therefore considered as a good alternative to other influence matrix algorithms based on the global influence matrix formulation (GIM method or algorithm of Raspo (2003)) if decomposition into a higher number of subdomains is considered.

6. Summary

New multi-domain algorithms were presented for solution of the energy and Navier-Stokes equations using the vorticity-streamfunction formulation based on the iterative domain decomposition scheme and the influence matrix technique. The influence matrix method was applied to treat the lack of boundary condition for vorticity at the physical boundary $\partial\Omega$ of the computational domain Ω.

The unknown coefficients ξ (unknown values of vorticity) were evaluated at the boundary of the computational domain applying the following algorithms: the global influence matrix technique (GIM method) and the iterative method based on the solution to the local system of equations in each subdomain (LIM method). The first method based on formulation of the global system of equations can be effectively applied for solution of the problems

where decomposition into a small number of subdomains is considered. The inversion of the global influence matrix can be done in the preprocessing stage on the master processor allowing one to evaluate the unknown coefficients at each time-cycle by simple matrix multiplication. The collective communication between the master and other processors was applied in that case. In the second algorithm, the local influence matrices were formulated and inversed locally in each subdomain in the preprocessing stage, while at each time-cycle the unknown coefficients were obtained using the iterative influence matrix where the "point-to-point" communication procedures were applied for data transmission between the processors.

The accuracy of both algorithms was checked for solution of the benchmark driven cavity problems, and finally some solutions to the natural convection problem in tall cavity were presented splitting the computational domain into $N_{el} = 10$ subdomains in one space direction. Good agreement with the benchmark results were obtained for the solution to the monodomain and multidomain problems confirming correctness of the influence matrix and domain decomposition methods implementation.

The parallel performance of the iterative influence matrix methods were analysed for solution of the natural convection problem, and it was shown that the computational time obtained using the LIM method was smaller than applying the GIM algorithm if the decomposition into a higher number of subdomains was considered (running the algorithm on a higher number of processors). The former algorithm can be then considered as a good alternative to the global influence matrix formulations if the solution to the problems involving both spectral approximation and the multi-domain technique is considered.

Acknowledgement

The research work was supported by Polish Ministry of Education and Science under the grant No. 4 T07A 016 26 "Parallel computing in the analysis of the Navier-Stokes equations using spectral methods".

References

1. Bayliss A., Class A., Matkowsky B.J., 1994, Roundoff error in computing derivatives using Chebyshev differentiation matrix, *J. of Comput. Physics*, **116**, 380-383

2. Canuto C., Hussaini M.Y., Quarteroni A., 1988, *Spectral Methods in Fluid Dynamics*, Springer-Verlag, New York

3. Ehrenstein U., Peyret R., 1986, A collocation Chebyshev method for solving Stokes-type equations, In: Bristeau M.O., Glowinski R., Hauguel A., Périaux J. (Eds.), *Sixth Int. Symp. Finite Elements in Flow Problems*, INRIA, 213-218

4. Ehrenstein U., Peyret R., 1989, A collocation Chebyshev method for the Navier-Stokes equations with application to double-diffusive convection, *Int. J. Numer. Methods Fluids*, **9**, 427-452

5. Forestier M.Y., Pasquetti R., Peyret R., Sabbah C., 2000, Spatial development of wakes using a spectral multi-domain technique, *Appl. Numer. Math.*, **33**, 207-216

6. Ghia U., Ghia K.N., Shin C.T., 1982, High-Re solutions for compressible flow using the Navier-Stokes equations and multigrid method, *J. of Comput. Phys.*, **48**, 387-411

7. Haidvogel D.B., Zang T.A., 1979, The accurate solution of Poisson's equation by expansion in Chebyshev polynomials, *J. of Comput. Phys.*, **30**, 167-180

8. Haldenwang P., Labrosse G., Abboudi S., 1984, Chebyshev 3-D spectral and 2-D pseudospectral solvers for the Helmholtz equation, *J. of Comput. Phys.*, **55**, 115-128

9. Hugues S., Randriamampianina A., 1998, An improved projection scheme applied to pseudospectral methods for the incompressible Navier-Stokes equations, *Int. J. Numer. Meth. Fluids*, **28**, 501-521

10. Isaacson E., Keller H.B., 1966, *Analysis of Numerical Methods*, J. Wiley and Sons, New York

11. Kleiser L., Schumann U., 1980, Treatment of incompressibility and boundary conditions in 3D numerical spectral simulations of plane channels flows, In: *Proc. 3rd GAMM Conf. Numerical Methods in Fluid Mechanics, Notes on Numerical Fluid Mechanics*, **2**, Vieweg, Braunschweig, 165-173

12. Kubacki S., 2005, *Parallel Computing in the Analysis of the Navier-Stokes Equations Using Spectral Methods*, Ph.D. Thesis, Czestochowa Univ. of Technology, Czestochowa [in Polish]

13. Louchart O., Randriamampianina A., 2000, A spectral iterative domain decomposition technique for the incompressible Navier-Stokes equations, *Appl. Numer. Math.*, **33**, 233-240

14. Louchart O., Randriamampianina A., Leonardi E., 1998, Spectral domain decomposition technique for the incompressible Navier-Stokes equations, *Numer. Heat Transfer, Part A.*, **34**, 495-518

15. Peyret R., 2002, *Spectral Methods for Incompressible Viscous Flow*, Springer-Verlag, New York

16. Raspo I., 2003, A direct spectral domain decomposition method for computation of rotating flows in T-shape geometry, *Comput and Fluids*, **32**, 431-456

17. Sabbah C., Pasquetti R., 1998, A divergence-free multidomain spectral solver of the Navier-Stokes equations in geometries of high aspect ratio, *J. of Comput. Phys.*, **139**, 359-379

18. Sabbah C., Pasquetti R., Peyret R., Levitsky V., Chaschechkin Y.D., 2001, Numerical and laboratory experiments of sidewall heating thermohaline convection, *Int. J. Heat Mass Transfer*, **44**, 2681-2697

19. Tuckerman L., 1989, Divergence-free velocity field in non periodic geometries, *J. of Comput. Phys.*, **80**, 403-441

20. Vanel J.M., Peyret R., Bontoux P., 1986, A pseudospectral solution of vorticity-streamfunction equations using the influence matrix method, In: Morton K.W., Baines M.J. (Eds.), *Numerical Methods Fluid Dynamics*, **II**, Clarendon, Oxford, 463-475

Zastosowanie metody macierzy wpływu w połączeniu z metodą dekompozycji obszaru obliczeniowego do rozwiązania równań Naviera-Stokesa sformułowanych w postaci wirowość-funkcja prądu

Streszczenie

W pracy przedstawiono nowy iteracyjny algorytm dekompozycji obszaru obliczeniowego oparty na metodzie macierzy wpływu w zastosowaniu do równań Naviera-Stokesa dla przepływu czynnika nieściśliwego w sformułowaniu wirowość-funkcja prądu. Spektralna metoda kolokacji wykorzystująca szeregi wielomianów Czebyszewa oraz metoda macierzy wpływu została zastosowana do rozwiązania zagadnienia Stokesa, będącego rezultatem dyskretyzacji równań Naviera-Stokesa w funkcji czasu, w każdym z podobszarów obszaru obliczeniowego, natomiast warunek ciągłości rozwiązania i jego pierwszej pochodnej na powierzchniach rozdziału pomiędzy podobszarami został uzyskany przy pomocy metody iteracyjnej.

Manuscript received April 7, 2008; accepted for print October 3, 2008